

Metastable Angular Distributions from Electron-Stimulated Desorption

Mark D. Alvey, Miles J. Dresser,^(a) and John T. Yates, Jr.

Surface Science Center, Department of Chemistry, University of Pittsburgh, Pittsburgh, Pennsylvania 15260

(Received 31 July 1985)

We have, for the first time, measured by electron-stimulated desorption the angular distribution of electronically excited (metastable) species from CO adsorbed on Ni(110). The angular distribution of metastable desorption is strongly peaked in the normal direction, as is also found for ionic desorption products. This indicates that the metastable is repelled along the direction of the bond being broken. We also observe an asymmetry in the azimuthal angular distribution which is correlated with the substrate crystal structure. The metastable exhibits a maximum in its yield versus coverage.

PACS numbers: 79.20.Kz, 68.45.Da

The angular distributions of positive ions¹ and ground-state neutrals² desorbing as a result of electron impact have been measured in the past, but the angular distribution of electronically excited neutrals (metastables) desorbing as a result of electron impact has not been previously reported. In this work we show that the metastable fragments from CO molecules adsorbed on ridge Ni atoms on Ni(110)³ form a distribution that is sharply peaked in the direction normal to the surface, has an ellipticity in its azimuthal profile, and has a strong dependence of yield on coverage.

The apparatus used has been discussed previously,^{4,5} but is modified for these experiments as shown in Fig. 1(a). Electrons (300 eV) are directed to the crystal surface in a beam about 1 mm in diameter. These incident electrons are scattered from the clean surface, produce secondary electrons, and induce excitations that lead to a characteristic soft x-ray photon background.⁴ If there is an adsorbed layer on the surface, these incident electrons may also cause stimulated desorption that leads to the release of ionic, ground-state neutral, or excited neutral particles. In this experiment the bias voltages between the sample and the four grids are chosen to prohibit the passage of charged particles. Neutral particles can then pass through the grids to the microchannel plate (MCP). Ground-state neutrals do not have sufficient energy to excite the MCP (typically less than 2 eV of kinetic energy⁶); however, metastable species frequently have sufficient electronic energy to excite the MCP upon collision with its surface. Each metastable particle produces a burst of electrons at the resistive anode (a position-sensitive detector mounted behind the MCPs). The position computer sends to the multichannel analyzer (MCA) a pair of pulses proportional to the (X, Y) coordinates of the metastable point of impact on the MCP. These events are stored by the MCA until a full distribution is evident (typically 10^6 counts). Angular calibration across the detector screen was accomplished by rotating the crystal to different positions and recording the distribution; this calibration agrees with the known apparatus geometry. This apparatus is contained in an ultrahigh-vacuum cham-

ber of base pressure 2×10^{-11} Torr. The chamber is also equipped for low-energy electron diffraction, Auger analysis, ion sputtering, mass spectrometry, and calibrated beam dosing.⁵ The crystal can be heated to above 1000 K (typical cleaning and annealing was done at 970 K). CO adsorption, and all measurements,

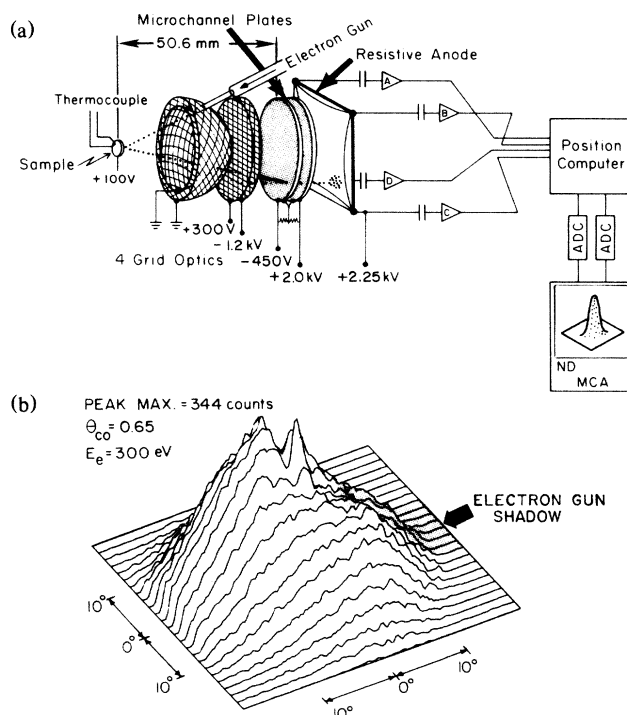


FIG. 1. (a) Schematic diagram of the angular distribution apparatus with digital acquisition. The distance from sample to first microchannel plate is 50.6 mm. Because of the exploded diagram the electron-gun drift tube does not appear to intrude on the region of data acquisition as much as is experimentally observed. (b) Acquired data for $\theta = 0.65$ CO/Ni(110) at 83 K; grids biased to prevent charged-particle passage. The soft x-ray photon background has been subtracted. The region where the electron gun appears to interfere with the data is shaded and indicated as the electron-gun shadow. A small dead spot (reduced MCP gain) exists near the end of the electron-gun shadow.

were carried out at 83 K.

A metastable angular distribution is shown in Fig. 1(b), for an electron current $I_e = 1.00 \times 10^{-8}$ A. These data were acquired in ~ 175 s which, with dead-time corrections for both the position computer and the MCA, corresponded to ~ 120 s live acquisition time. The data are stored in a 128×128 array. To generate the plot of Fig. 1(b), every fifth row of data is averaged with its nearest and next-nearest neighbor rows to produce the lines shown. The data of Fig. 1(b) have also had the soft x-ray background subtracted.⁷

Further to justify that the observed distribution is due to metastable particles, we performed a time-of-flight experiment. The electron gun was pulsed with a pulse width of $1.5 \mu\text{s}$ and a repeat time of $140 \mu\text{s}$. The MCA could be gated on for $1.2 \mu\text{s}$ with arbitrary delay after the electron pulse. The counts thus accumulated generated a pattern similar to that of Fig. 1(b) although its signal-to-noise ratio is smaller. Photon flight times are less than 1 ns, so that they cannot contribute to this pattern, which was acquired for delays greater than $8 \mu\text{s}$ after the electron pulse. Kinetic energy distributions of the metastable fragment from a CO layer on Ru(001)⁶ and W(100)⁸ surfaces have been reported and are almost identical to each other in average energy and breadth. If we use those values to estimate the average metastable flight time in our configuration, we predict that the peak of the flight distribution is $13 \mu\text{s}$ and the half-maximum intensities occur at 9 and $24 \mu\text{s}$. In our measurements, the greatest number of counts was observed $14 \mu\text{s}$ from the leading edge of the electron pulse. Our configuration is not optimum for precise time-of-flight measurements because of an 11% variation in flight-path length to different parts of the MCP. There is sufficient resolution to determine that our neutral is traveling with a very similar energy/mass ratio to that of those previously reported.^{7,8}

The angular distribution of the metastables is displayed in two other formats (Fig. 2) in order to demonstrate salient features. Figure 2(a) is a contour plot of the distribution showing lines of constant intensity (count). The asymmetry of the azimuthal distribution is most evident here. The beam contour has a broader spread in the $[1\bar{1}0]$ Ni surface direction than it does in the $[001]$ direction. Note that contour *c* is at half of the peak intensity and contour *d* is at $1/e$ of the peak intensity. Our best measurement of the distribution width is the full width at $1/e$ of the maximum intensity ($\text{FW}e^{-1}\text{M}$) since that contour in the principal directions is not complicated by the gun shadow. The $\text{FW}e^{-1}\text{M}$ in the $[001]$ direction is $19^\circ \pm 1^\circ$ and in the $[1\bar{1}0]$ direction it is $24^\circ \pm 1^\circ$. This gives an ellipticity ratio ($\epsilon = \text{minor axis}/\text{major axis}$) of $\epsilon = 0.8$.

If the data are cut with a plane parallel to the Z axis (perpendicular to the plane of the MCP) and parallel

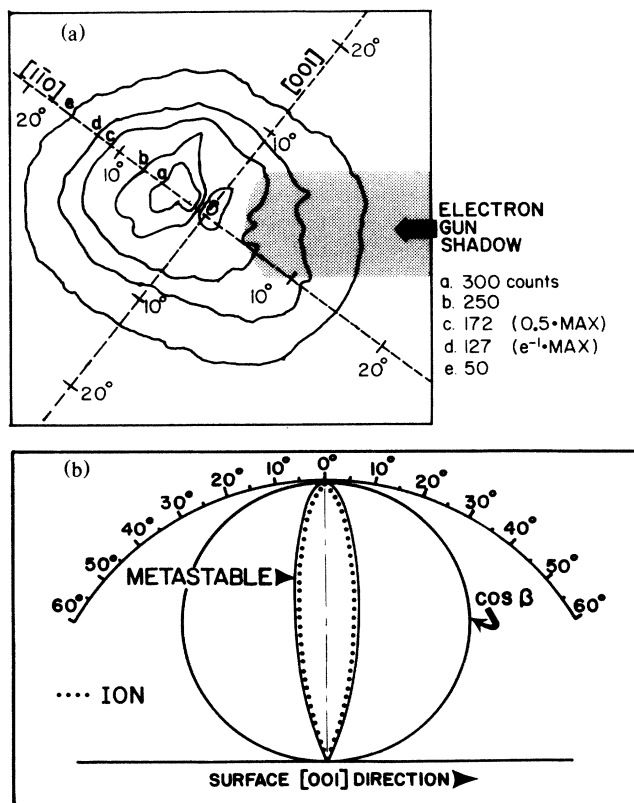


FIG. 2. (a) The data of Fig. 1(b) presented in a contour plot to show the elongation of the metastable beam in the azimuth parallel to the $[110]$ ridges of the Ni substrate. (b) A polar plot of the same data in a cut parallel to the $[001]$ surface direction through the maximum in the data. A $\cos\beta$ and ionic distribution are also shown for comparison.

to the $[001]$ direction intersecting the maximum of the distribution outside of the gun shadow, two-dimensional profiles are generated that allow comparison of some important features of our distribution. Figure 2(b) shows such a cut replotted as a polar plot. The strongly peaked character of the metastable angular distribution is seen most definitively here. For comparison we show the $\cos\beta$ distribution, which is characteristic of neutral CO thermal desorption from Ni(110),⁹ and the positive-ion distribution from our surface (normalized to the metastable intensity). With this comparison it is evident that our metastable angular distribution is very similar to the sharply peaked ion angular distribution. Feulner, Riedl, and Menzel² have reported the angular distribution of ground-state neutrals produced by electron impact on CO on Ru(001). They find those particles to have a significantly narrower angular distribution than for the thermal desorption process, but their distribution is much broader than ionic distributions. While our ionic products consist of CO^+ and O^+ ions (we estimate 40% and 60%, respectively, using mass spectrometry), we

note that CO^+ and O^+ angular distributions are very similar. For example on Ni(110) at $\theta = 0.75$ CO/Ni, Riedl and Menzel¹⁰ have shown that the FWHM for O^+ (with 280-eV electrons) is 17.3° in the [110] direction and 20.8° in the [001] direction at 90 K. The corresponding values for CO^+ are 16° in the [110] and 15° in the [001] direction. Our ionic pattern is obtained by a difference of the pure metastable pattern and one biased to permit passage of the positive ions also (but with no crystal bias). Our FWHM for ions in the [001] azimuth is $15^\circ \pm 3^\circ$.

The coverage dependence of the metastable angular profile was also studied. Figure 3(a) shows a series of cuts, as described previously for the polar plot, for various coverages of CO. There is no significant observed change in the shape of these profiles, and there

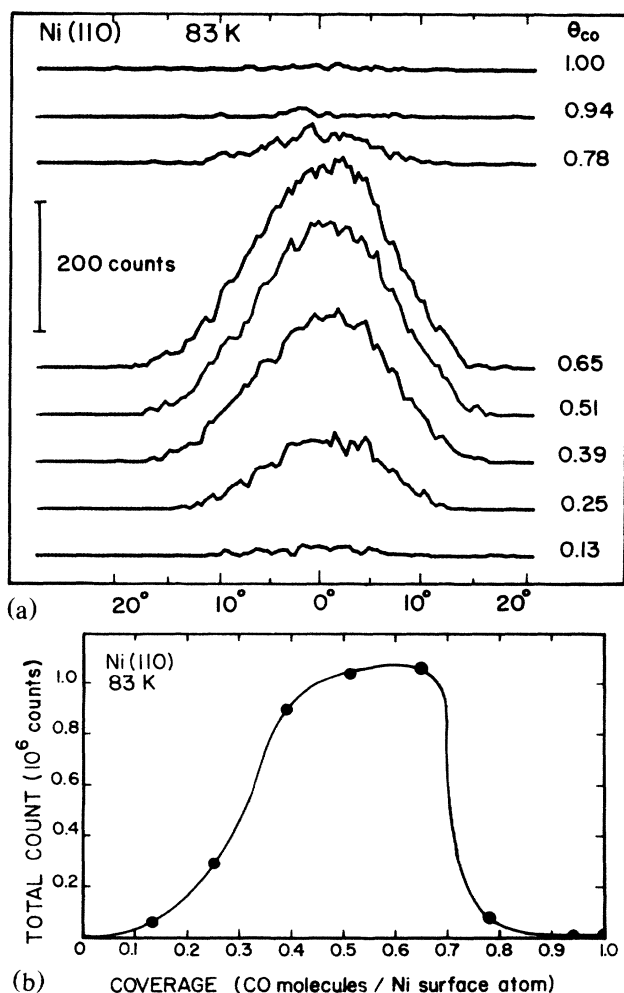


FIG. 3. (a) A series of cuts through the metastable angular distribution parallel to the [001] surface direction at the peak maximum. Each line represents a different CO coverage which is indicated to its right. (b) A plot of the total count integrated over the entire detector for different CO coverages.

is also no noticeable change in the shape of the full three-dimensional beam profile with coverage. We do, however, observe a striking variation in the amplitude of these distributions with CO coverage. The amplitude rises monotonically up to $\theta \cong 0.65$ CO/Ni, at which point it drops rapidly toward zero as coverage increases. The effect is also seen in the variation of the total count integrated under the full distribution. These data are presented in Fig. 3(b) where the drop toward zero resembles the drop in ion intensity with increasing CO coverage reported previously by this group and others.^{11,12} Here, dramatic increases were seen in the yield of ions at high electron energy.^{11b,12} In the present work there was little difference in the metastable yields at 1000 V as compared to those we report here for 300-eV electrons.

A precise identification of the metastable species is not possible with our apparatus. The most likely candidates are $\text{CO}^*(a^3\pi)$ or $\text{O}^*(3^5S_0$ or $2^1S_0)$. In the case of CO on W(100), Sandstrom¹³ has resolved the issue by measuring the change in the time-of-flight distribution for two different flight-path lengths. From the change in distribution one can infer the lifetime of the metastable species. A lifetime of 0.8 ms was determined, which clearly identifies the species as $a^3\pi$ -CO.

The strong similarity of the energy distributions for the metastables from W(100) and Ru(001) suggests that perhaps $a^3\pi$ -CO is a common product of electron impact on chemisorbed CO.

These results suggest that the role of the bond direction is of primary importance in determination of the trajectory of the metastable. Two models are possible: (1) An ionic state is initially produced, and the initial acceleration is along the bond direction.¹ The ion is subsequently neutralized to an excited metastable species in the vicinity of the surface.¹⁴ (2) A metastable species is initially produced by electronic excitation of the CO molecule and escapes along the bond direction.

Correlation of these results for the metastable angular distribution with other work is possible. It is well known for ionic desorption in electron-stimulated desorption that there is a close correspondence between the ion-ejection direction and the direction of the bond being broken.¹⁵ Riedl and Menzel¹⁰ have shown that little asymmetry exists in the CO^+ azimuthal profile from CO/Ni(110); the O^+ azimuthal profile is broadened in the [001] directions. Model (1) above is consistent with the metastable's being derived from CO^+ by means of a neutralization process which is more efficient over the Ni atom rows to produce enhanced metastable yields in the $[1\bar{1}0]$ direction. Model (2) is consistent with the idea that at intermediate CO coverages, the Ni—CO bond direction for the CO molecules on ridge Ni atoms is distributed such

that slight inclination in some of the Ni—CO bonds occurs in the $[1\bar{1}0]$ directions as a result of intermolecular repulsion. This could occur at the ends of short linear chains of CO on the Ni ridges. The significant drop in metastable yield at a coverage of $\theta \cong 0.7$ CO/Ni is consistent with intermolecular quenching processes between CO molecules, as originally proposed by Netzer and Madey¹⁶ for CO on Ni(111).

We have shown that the metastable emission from a CO layer on Ni(110) under electron bombardment is strongly peaked in the direction normal to the surface (probably the Ni—CO bond direction). The angular distribution is somewhat elliptical in the azimuthal projection with the long axis parallel to the rows of nickel surface atoms. The metastable angular distribution is almost as sharp as ionic distributions,¹⁰ and is much more strongly peaked than for ground-state neutrals derived from electron impact,² and from CO thermally desorbing from Ni(110).⁹ The CO coverage dependence of metastable yield is similar to that for ion production from CO layers with low-energy excitation. The yield of metastable species is not enhanced at high excitation energies as is the case for O⁺ emission. These observations lead to the view that the adsorbed CO is excited by an electronic transition to a repulsive ionic state or a repulsive metastable state, which desorbs in a sharply peaked angular distribution centered about the direction of the bond being broken. Data of other workers suggest that this metastable is a $^3\pi$ -CO.

We thank Dr. T. E. Madey and Dr. W. Clinton for helpful comments on this work. This work was supported by the Air Force Office of Scientific Research under Contract No. 82-0133.

^(a)Present address: Department of Physics, Washington State University, Pullman, Wash. 99164.

¹J. J. Czyzewski, T. E. Madey, and J. T. Yates, Jr., Phys. Rev. Lett. **32**, 777 (1974).

²P. Feulner, W. Riedl, and D. Menzel, Phys. Rev. Lett. **50**, 986 (1983).

³J. Behm, G. Ertl, and V. Penka, Surf. Sci. **160**, 387 (1985).

⁴M. J. Dresser, M. D. Alvey, and J. T. Yates, Jr., Surf. Sci. (to be published).

⁵C. Klauber, M. D. Alvey, and J. T. Yates, Jr., Surf. Sci. **154**, 139 (1985).

⁶P. Feulner, D. Menzel, H. J. Kreuzer, and Z. W. Gortel, Phys. Rev. Lett. **53**, 671 (1983).

⁷The justification for this procedure is the subject of another paper (Ref. 4). We acquire the photon background from the clean crystal surface. Soft x-ray appearance potential spectroscopy has shown that adsorbed layers only make subtle changes in the total x-ray yield (for example, one differentiates the appearance potential spectroscopy yield to make the contributions of an adsorbed layer more visible). Also, the soft x-ray angular distribution that we have measured is a very broad featureless pattern so that the strongly peaked features we see in our neutral patterns are not easily confused with the photon background.

⁸I. G. Newsham, J. V. Hogue, and D. R. Sandstrom, J. Vac. Sci. Technol. **9**, 596 (1972), and **10**, 39 (1973).

⁹H. P. Steinruck, A. Winkler, and K. D. Rendulic, J. Phys. C, **17**, L311 (1984).

¹⁰W. Riedl and D. Menzel, in *Desorption Induced by Electronic Transitions, DIET II*, edited by W. Brenig, and D. Menzel, Springer Series in Surface Sciences Vol. 4 (Springer-Verlag, Berlin, 1985), p. 136.

^{11a}J. Lee, J. Arias, C. Hanrahan, R. Martin, H. Metiu, C. Klauber, M. D. Alvey, M. J. Dresser, and J. T. Yates, Jr., Surf. Sci. **159**, L460 (1985).

^{11b}M. D. Alvey, M. J. Dresser, and J. T. Yates, Jr., Surf. Sci. (to be published).

¹²W. Riedl, and D. Menzel, to be published.

¹³D. R. Sandstrom, M. J. Dresser, and W. Dong, to be published.

¹⁴D. Menzel and R. Gomer, J. Chem. Phys. **41**, 3311 (1964).

¹⁵T. E. Madey, F. P. Netzer, J. E. Houston, D. M. Hanson, and R. Stockbauer in *Desorption Induced by Electronic Transitions, DIET I*, edited by N. H. Tolk, M. M. Traum, T. E. Madey, and J. C. Tully, Springer Series in Chemical Physics Vol. 24 (Springer-Verlag, Heidelberg, 1983), p. 120.

¹⁶F. P. Netzer and T. E. Madey, J. Chem. Phys. **76**, 710 (1982).

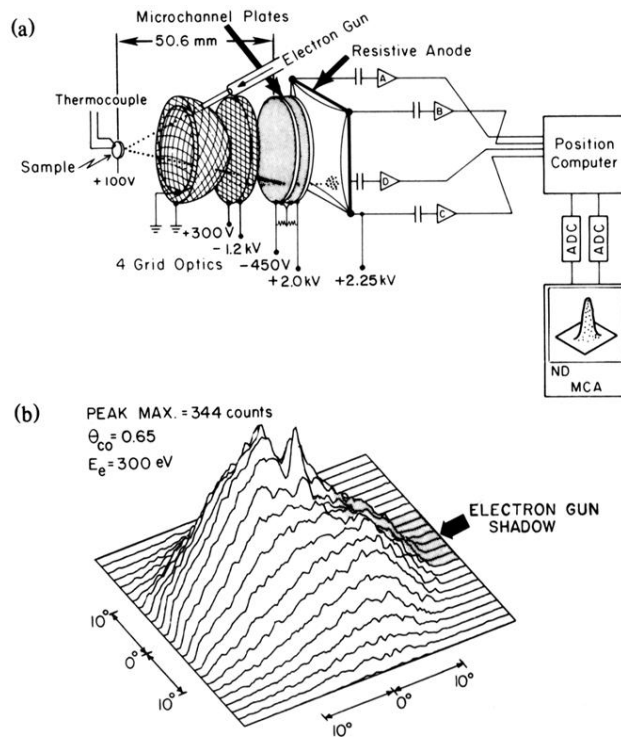


FIG. 1. (a) Schematic diagram of the angular distribution apparatus with digital acquisition. The distance from sample to first microchannel plate is 50.6 mm. Because of the exploded diagram the electron-gun drift tube does not appear to intrude on the region of data acquisition as much as is experimentally observed. (b) Acquired data for $\theta = 0.65$ CO/Ni(110) at 83 K; grids biased to prevent charged-particle passage. The soft x-ray photon background has been subtracted. The region where the electron gun appears to interfere with the data is shaded and indicated as the electron-gun shadow. A small dead spot (reduced MCP gain) exists near the end of the electron-gun shadow.

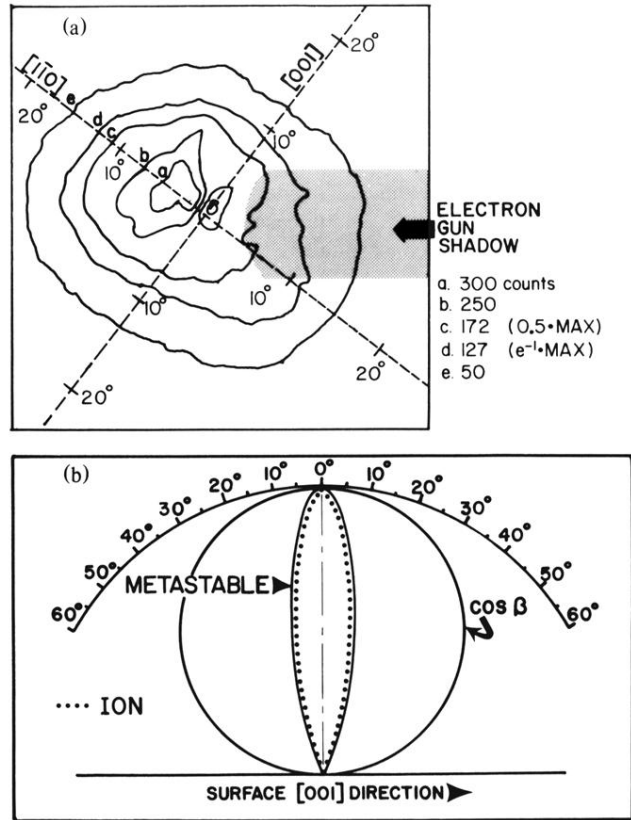


FIG. 2. (a) The data of Fig. 1(b) presented in a contour plot to show the elongation of the metastable beam in the azimuth parallel to the [110] ridges of the Ni substrate. (b) A polar plot of the same data in a cut parallel to the [001] surface direction through the maximum in the data. A $\cos\beta$ and ionic distribution are also shown for comparison.